

Detecting the Beaming Effect of Gravitational Waves

Alejandro Torres-Orjuela and Xian Chen*

Astronomy Department, School of Physics, Peking University, 100871 Beijing, China and Kavli Institute for Astronomy and Astrophysics at Peking University, 100871 Beijing, China

Zhoujian Cao

Institute of Applied Mathematics, Academy of Mathematics and Systems Science, Chinese Academy of Sciences, Beijing 100190, China

Pau Amaro-Seoane

*Institute of Space Sciences (ICE, CSIC) & Institut d'Estudis Espacials de Catalunya (IEEC) at Campus UAB, 08193 Barcelona, Spain
Institute of Applied Mathematics, Academy of Mathematics and Systems Science, Chinese Academy of Sciences, Beijing 100190, China
Kavli Institute for Astronomy and Astrophysics at Peking University, 100871 Beijing, China and Zentrum für Astronomie und Astrophysik, TU Berlin, 10623 Berlin, Germany*

Peng Peng

*Astronomy Department, School of Physics, Peking University, 100871 Beijing, China
(Dated: July 24, 2022)*

The models currently used in the detection of gravitational waves (GWs) either do not consider a relative motion between the center-of-mass of the source and the observer, or usually only consider its effect on the frequencies of GWs. However, it is known for light waves that a relative motion not only changes the frequencies but also the brightness of the source, the latter of which is called the “beaming effect”. Here we investigate such an effect for GWs and find that the observed amplitude of a GW signal, unlike the behavior of light, is not a monotonic function of the relative velocity and responds differently to the two GW polarizations. We attribute the difference to a rotation of the wave-vector, as well as a reorientation of the GW polarizations. We find that even for velocities as small as 0.25% of the speed of light, ignoring the aforementioned beaming effect could induce a systematic error that is larger than the designated calibration accuracy of LIGO. This error could lead to an incorrect estimation of the distance and orbital inclination of a GW source, or result in a spurious signal that appears to be incompatible with general relativity.

PACS: 04.80.Nn; 04.30.Nk; 95.55.Ym

I. INTRODUCTION

The direct detection of gravitational waves (GWs) by the ground-based observatories LIGO and Virgo [1, 2] has led in the last few years to the advent of data-driven gravitational wave astronomy. A key ingredient in the detections is the success of numerical relativity to reproduce the inspiral, merger, and ringdown waveforms of compact binaries, such as binary black holes (BBHs, e.g. [3–5]). In alliance with various inspiral modelling methods (e.g. [6–9]), these waveform templates have allowed us to extract from the observed signals physical parameters for the binaries, such as the masses of the compact objects and their spins.

Although the templates are computed in a coordinate system where the center-of-mass (CoM) of the source is at rest, observations are conducted in a different frame, where the detectors are at rest. The two frames, in general, are not equal because astrophysical objects move

relative to us. As a result, the computed and the observed waveforms may differ. Indeed, recent works considered the astrophysical scenarios in which the sources are moving at a non-relativistic velocity and showed that if the velocity varies with time, the acceleration could induce a detectable difference in the observed waveform, by shifting the GW frequency (the Doppler effect [10–14]) or changing the way the high-order GW modes interact [15].

The difference should be the most prominent when the relative velocity approaches the speed of light, c . This case, however, is not considered in the previous studies. The main reason is that gaining a relativistic velocity is considered difficult for BBHs in normal astrophysical environments [16, 17].

This conventional view, however, is no longer complete. Recent studies showed that BBHs could merge more rapidly in the center of a galaxy, especially in the presence of a supermassive black hole (SMBH). The mergers are caused by either the tidal perturbation by the SMBH [18–27] or the hydrodynamical friction against an accretion disk, if the SMBH is in an active galactic nucleus (AGN, e.g. [28–32]). In particular, as we found recently, a small fraction of the mergers could happen within a

* Corresponding author: xian.chen@pku.edu.cn

distance of ten Schwarzschild radii of a SMBH [33–35]. Consequently, the CoM of the BBHs would move at a velocity of $\mathcal{O}(c/\sqrt{20})$ relative to a distant observer.

If BBHs gain such a relativistic velocity, the power of the GWs, when viewed in the rest frame of the detector, should, in principle, appear beamed in the direction of the motion. Such a “beaming effect” is well known for light waves [36, 37] but not as well understood for GWs. Theoretically, the standard equation for the generation of GWs assumes a slow motion for the source [38, 39], and hence is not easily generalizable to account for a relativistic velocity. A self-consistent treatment of the problem should, instead, consider a source which extends into its own wave zone, but the resulting equation is difficult to solve, except for a few special cases [40].

One possibility of simplifying the calculation is to return to the GW strain previously computed in the rest frame of the source and Lorentz transform it into the rest frame of the detector. This operation, although theoretically appropriate, may result in an observational issue, especially for BBHs, because the Lorentz transformation changes the apparent direction of the GW polarization [41]. This direction is used to infer the orientation of the orbit of a BBH [42], which is particularly useful to constrain the orbital precession, black-hole spin, or alternative gravity theories [43].

To overcome the above difficulties, we take a different approach towards addressing the beaming effect of GWs. We stay in the rest frame of the source and investigate the response of a moving detector to the GW background. The advantage of this approach is that one can use our response function (equivalent to an “antenna pattern”) to extract the GW waveform in the source frame. This waveform can be compared directly with the templates from numerical relativity to infer correct physical parameters of the source, including the orientation of the orbit. Throughout this paper, we use $G = c = 1$.

II. THE BASIC SCENARIO

We first revisit the textbook example in which a pulse of light is sent out by an emitter, reflected back by a mirror, and we measure the duration of the round trip of the light (e.g. [44]). This example has the advantage of laying bare the fundamentals of interferometric techniques as used in real detectors such as LIGO/Virgo [45] and the Laser Interferometer Space Antenna (LISA [46]). However, the textbook formulae are derived assuming that there is no relative motion between the detector and the CoM of the source. This assumption no longer holds in our problem, and hence in this section we generalize the formulae.

We choose a coordinate system (t, x, y, z) at rest with respect to the CoM of the GW source. This allows us to adopt the standard formulae for GW radiation [38, 39]. Furthermore, we (i) expand the spacetime metric to linear order, (ii) adopt the *transverse-traceless* (TT)

gauge condition [47], and (iii) set the wave-vector \mathbf{k} of the GW in the z -direction and the $+$ -polarization in the direction of the x, y coordinates. With these standard considerations, the spacetime metric far away from the GW source reduces to

$$g_{\mu\nu} = \eta_{\mu\nu} + h_{\mu\nu}, \quad (1)$$

where $\eta_{\mu\nu} := \text{diag}(1, -1, -1, -1)$ is the Minkowski metric and $h_{\mu\nu}$ represents the GW. More specifically, the only non-vanishing components of $h_{\mu\nu}$ are

$$h_{xx} = -h_{yy} = h_+^\omega(t, z) \text{ and } h_{xy} = h_{yx} = h_\times^\omega(t, z). \quad (2)$$

To simplify the problem, we focus on only one harmonic, where we denote its frequency as ω and its amplitude as h_0 . Suppose the relative strength of the two polarizations are ϵ_+ and ϵ_\times , we then can write

$$h_{+,\times}^\omega(t, z) = \epsilon_{+,\times} h_0 e^{i(\omega t - kz)}, \quad (3)$$

where i is the imaginary unit and $\omega = k$ in natural units. We note that in the standard case of a circular binary, $\epsilon_{+,\times}$ only depend on the angle between the angular momentum of the orbit and the line of sight of the observer [48]. All the above quantities are measured in the rest frame of the source.

Suppose the electromagnetic pulse sets off at the time t_s from the location of the emitter $\mathbf{p}_E(t_s)$, bounces back at the time t_r by the reflector located at $\mathbf{p}_R(t_r)$, and finally returns to the emitter at $\mathbf{p}_E(t_e)$ at the time t_e . While in the textbook example the above spatial vectors are constant, in our case where both the emitter and the reflector are moving, these vectors are functions of time. Given this difference, we want to calculate the duration it takes, i.e., $t_e - t_s$, for the pulse to finish the round trip.

Since light travels along null geodesics, we use $g_{\mu\nu} dx^\mu dx^\nu = 0$ to compute the light travel time. Expanding the line element to linear order of h , we derive

$$dt = \sqrt{dx^2 + dy^2 + dz^2} - \frac{1}{2} \frac{1}{\sqrt{dx^2 + dy^2 + dz^2}} \times [F_+(dx, dy)h_+^\omega(t, z) + F_\times(dx, dy)h_\times^\omega(t, z)], \quad (4)$$

where we have introduced the “response patterns” as

$$F_+(a, b) := (a^2 - b^2) \text{ and } F_\times(a, b) := 2ab. \quad (5)$$

Integrating Eq. (4) using the boundaries $\mathbf{p}_E(t_s)$, $\mathbf{p}_R(t_r)$, and $\mathbf{p}_E(t_e)$, we find

$$t_e - t_s = \int_{\mathbf{p}_E(t_s)}^{\mathbf{p}_R(t_r)} \left(\sqrt{dx^2 + dy^2 + dz^2} - \frac{1}{2} \frac{P(dx, dy)}{\sqrt{dx^2 + dy^2 + dz^2}} h^\omega(t, z) \right) + \int_{\mathbf{p}_R(t_r)}^{\mathbf{p}_E(t_e)} \left(\sqrt{dx^2 + dy^2 + dz^2} - \frac{1}{2} \frac{P(dx, dy)}{\sqrt{dx^2 + dy^2 + dz^2}} h^\omega(t, z) \right). \quad (6)$$

In the last equation we have adopted for compactness $h^\omega(t, z) := h_0 e^{i(\omega t - kz)}$ and

$$P(a, b) := \epsilon_+ F_+(a, b) + \epsilon_- F_-(a, b). \quad (7)$$

Our calculation of the integrals in Eq. (6) involves a linear parameterization of the geodesic of the light. For example, to calculate the first integral in Eq. (6), which we denote as I_1 , we first notice that the arm length L of LIGO or LISA is much shorter than the corresponding GW wavelength λ , i.e., we have $L/\lambda \ll 1$ (see e.g. [45, 46]). Consequently, we can linearize the geodesic as

$$\begin{pmatrix} t \\ \phi \end{pmatrix} = \begin{pmatrix} \beta^0 \\ \boldsymbol{\beta} \end{pmatrix} \xi + \begin{pmatrix} \gamma^0 \\ \boldsymbol{\gamma} \end{pmatrix}, \quad (8)$$

where ϕ are the three spacial components of the null geodesic of the light. Assuming that the two boundaries of the integration correspond to two values ξ_a and ξ_b , we can write

$$\begin{pmatrix} t_s \\ \mathbf{p}_E(t_s) \end{pmatrix} = \begin{pmatrix} \beta^0 \\ \boldsymbol{\beta} \end{pmatrix} \xi_a + \begin{pmatrix} \gamma^0 \\ \boldsymbol{\gamma} \end{pmatrix}, \quad (9a)$$

$$\begin{pmatrix} t_r \\ \mathbf{p}_R(t_r) \end{pmatrix} = \begin{pmatrix} \beta^0 \\ \boldsymbol{\beta} \end{pmatrix} \xi_b + \begin{pmatrix} \gamma^0 \\ \boldsymbol{\gamma} \end{pmatrix}. \quad (9b)$$

From these conditions the parameters β^0 , $\boldsymbol{\beta}$, γ^0 and $\boldsymbol{\gamma}$ can be determined as

$$\begin{pmatrix} \beta^0 \\ \boldsymbol{\beta} \end{pmatrix} = \frac{1}{\xi_b - \xi_a} \begin{pmatrix} t_r - t_s \\ \mathbf{p}_R(t_r) - \mathbf{p}_E(t_s) \end{pmatrix}, \quad (10a)$$

$$\begin{pmatrix} \gamma^0 \\ \boldsymbol{\gamma} \end{pmatrix} = \begin{pmatrix} t_r \\ \mathbf{p}_R(t_r) \end{pmatrix} - \begin{pmatrix} \beta^0 \\ \boldsymbol{\beta} \end{pmatrix} \xi_b. \quad (10b)$$

Applying the parametrization in Eq. (8), the integral I_1 takes the form

$$I_1 = \int_{\xi_a}^{\xi_b} \left(\sqrt{\boldsymbol{\beta}^2} - \frac{1}{2} \frac{P(\beta^1, \beta^2)}{\sqrt{\boldsymbol{\beta}^2}} \right) \times h^\omega(\beta^0 \xi + \gamma^0, \beta^3 \xi + \gamma^3) d\xi. \quad (11)$$

It can be solved analytically using the mathematical tools prepared in App. A. Similarly, we can also solve the second integral in Eq. (6). Summing up the two integrals, we find

$$t_e - t_s = \left[\sqrt{(\mathbf{p}_R(t_r) - \mathbf{p}_E(t_s))^2} + \frac{1}{2} \left(\frac{P(x_R(t_r) - x_E(t_s), y_R(t_r) - y_E(t_s))}{\sqrt{(\mathbf{p}_R(t_r) - \mathbf{p}_E(t_s))^2}} \times i \frac{h^\omega(t_r, z_R(t_r)) - h^\omega(t_s, z_E(t_s))}{\omega(t_r - t_s) - k(z_R(t_r) - z_E(t_s))} \right) \right] + \left[\sqrt{(\mathbf{p}_E(t_e) - \mathbf{p}_R(t_r))^2} + \frac{1}{2} \left(\frac{P(x_E(t_e) - x_R(t_r), y_E(t_e) - y_R(t_r))}{\sqrt{(\mathbf{p}_E(t_e) - \mathbf{p}_R(t_r))^2}} \times i \frac{h^\omega(t_e, z_E(t_e)) - h^\omega(t_r, z_R(t_r))}{\omega(t_e - t_r) - k(z_E(t_e) - z_R(t_r))} \right) \right]. \quad (12)$$

One can verify the last equation by considering the textbook example in which the detector is at rest relative to the GW source. In this case we can write

$$\mathbf{p}_E(t) = \mathbf{0} \text{ and } \mathbf{p}_R(t) = L\hat{\mathbf{p}}, \quad (13)$$

where L is the arm length of the detector and $\hat{\mathbf{p}} = (\hat{x}, \hat{y}, \hat{z})$ is a unit vector pointing from the emitter to the reflector, both quantities defined in the rest frame of the source when there is no GW. The problem can be further simplified because of the following factors. First, the travel time of the light for the outbound and inbound trip can be approximated by

$$t_r - t_s = t_1(1 + \mathfrak{h}_1) \text{ and } t_e - t_r = t_2(1 + \mathfrak{h}_2), \quad (14)$$

where t_1 and t_2 denote the light travel times without GWs, and \mathfrak{h}_1 and \mathfrak{h}_2 are of the order of h . Second, because L/λ is small, we can expand h around t_s . To linear order (of L/λ and h) the result is

$$h^\omega(t_r, L\hat{\mathbf{z}}) \approx h^\omega(t_s) + i(\omega t_1 - kL\hat{\mathbf{z}})h^\omega(t_s), \quad (15a)$$

$$h^\omega(t_e) \approx h^\omega(t_s) + i\omega(t_1 + t_2)h^\omega(t_s), \quad (15b)$$

where $h^\omega(t)$ is shorthand for $h^\omega(t, 0)$. Third, when there is no relative motion the coordinate time and the proper time of the emitter are the same, L equals the arm length in the rest frame of the detector L_0 , and $t_1 = t_2 = L_0$. Under these circumstances, Eq. (12) reduces to

$$\tau_e - \tau_s = 2L_0 \left(1 - \frac{1}{2} \left[F_+(\hat{x}, \hat{y}) h_+^\omega(\tau_s) + F_-(\hat{x}, \hat{y}) h_-^\omega(\tau_s) \right] \right), \quad (16)$$

where τ_s (τ_e) is the proper time at the emitter when the pulse leaves (returns). This equation is equivalent to that derived in text books (e.g. [44]). The above result is coordinate-independent, because it is a proper time measured by the same clock.

III. THE EFFECT OF RELATIVE MOTION

Now we consider the effect induced by a relative velocity of $\mathbf{v} = (v_x, v_y, v_z)$ between the detector and the CoM of the source. Since we choose a coordinate system where the GW source is at rest, $h_{\mu\nu}$ has the same components as in Eq. (2). The problem reduces to solving the light travel time between the two ends of a moving detector. In this case, the response of the detector will differ fundamentally from Eq. (16) because the spatial coordinates of the emitter and reflector are no longer constant.

More specifically, their motion not only has a linear component, $\mathbf{v}t$, but also a non-linear one caused by the perturbation of GWs. We derive this latter component in App. B, which is based on the free-fall geodesic equations for the emitter and reflector up to linear order of h . The

resulting spatial coordinates of the geodesics are

$$\mathbf{p}_E(t) = \mathbf{v}t + \frac{i\alpha h^{\bar{\omega}}(t)}{\bar{\omega}(1-v_z)}, \quad (17a)$$

$$\mathbf{p}_R(t) = L\hat{\mathbf{p}} + \mathbf{v}t + \frac{i\alpha h^{\bar{\omega}}(t, L\hat{z})}{\bar{\omega}(1-v_z)}, \quad (17b)$$

where $\bar{\omega} := \omega(1-v_z)$ and

$$\boldsymbol{\alpha} := \begin{pmatrix} \frac{1}{2}v_x P(v_x, v_y) - (1-v_z)[\epsilon_+ v_x + \epsilon_\times v_y] \\ \frac{1}{2}v_y P(v_x, v_y) - (1-v_z)[\epsilon_\times v_x - \epsilon_+ v_y] \\ -\frac{1}{2}(1-v_z)P(v_x, v_y) \end{pmatrix}. \quad (18)$$

We note that $1-v_z$ enters the equations because for the detector $\omega - kv_z$ is the rate at which the GW phase changes.

Eqs. (17) indicate that the emitter and reflector wiggle as they advance along their geodesics. This wiggling can be understood from the fact that a four-velocity has always constant magnitude. Since GWs deform the metric, the four-velocity has to rearrange to preserve its magnitude, which in turn changes the direction of the trajectory. Moreover, Eq. (18) shows that when $v_x = v_y = 0$, the wiggling effect vanishes even if v_z is non-zero. This is because in TT-gauge the t - and z -components are not deformed by the GW.

A. The light travel time

Knowing $\mathbf{p}_E(t)$ and $\mathbf{p}_R(t)$, we can use them in Eq. (12) and derive the duration of the round trip for light. The calculation resembles that without velocity but with three differences. (i) The length of the arm, L , and the light travel times, t_1 and t_2 , differ from those in the previous paragraph by a coordinate transformation. (ii) The wiggling of the emitter and reflector changes the proper distance that light traverses. Effectively, this means the first-order terms in Eq. (14) contribute to the calculation of the first and third terms in Eq. (12). (iii) We want to derive the proper time of the emitter, not the coordinate time, because the latter is coordinate-dependent.

To proceed, we first calculate the light-travel times without GWs, which are

$$t_{1,2} = \gamma^2 L \left(\frac{1}{\gamma(\theta)} \pm v \cos(\theta) \right), \quad (19)$$

where $\gamma := (1-v^2)^{-1/2}$ is the Lorentz factor, $\gamma(\theta) := (1-v^2 \sin^2(\theta))^{-1/2}$, and θ is the angle spanned by the relative velocity and the arm of the detector, as seen in the rest frame of the source. The length of the arm in the source frame is

$$L = \frac{\gamma(\theta)}{\gamma} L_0. \quad (20)$$

Next, we calculate the four terms in Eq. (12). For the first and third terms, we simplify them by performing

three steps: (i) replace the times using the approximations specified in Eq. (14), (ii) Taylor expand the roots to linear order of h , and (iii) expand the h around t_s up to linear order of L/λ , like in Eqs. (15). Executing these steps, we find

$$\begin{aligned} \sqrt{(\mathbf{p}_R(t_r) - \mathbf{p}_E(t_s))^2} &= t_1(1 + \mathfrak{h}_1) - \frac{L}{\gamma(\theta)} \mathfrak{h}_1 \\ &+ \frac{h^{\bar{\omega}}(t_s)}{2\bar{\omega}} \left(\bar{\omega} - \frac{\omega L \hat{z}}{t_1} \right) \left[P(v_x, v_y) t_1 \right. \\ &+ \left. \left(2P(\hat{x}, \hat{y}, v_x, v_y) + \left(\hat{z} + \frac{1}{\gamma(\theta)} \right) \frac{P(v_x, v_y)}{1-v_z} \right) L \right], \end{aligned} \quad (21a)$$

$$\begin{aligned} \sqrt{(\mathbf{p}_E(t_e) - \mathbf{p}_R(t_r))^2} &= t_2(1 + \mathfrak{h}_2) - \frac{L}{\gamma(\theta)} \mathfrak{h}_2 \\ &+ \frac{h^{\bar{\omega}}(t_s)}{2\bar{\omega}} \left(\bar{\omega} + \frac{\omega L \hat{z}}{t_2} \right) \left[P(v_x, v_y) t_2 \right. \\ &- \left. \left(2P(\hat{x}, \hat{y}, v_x, v_y) + \left(\hat{z} - \frac{1}{\gamma(\theta)} \right) \frac{P(v_x, v_y)}{1-v_z} \right) L \right], \end{aligned} \quad (21b)$$

where we have applied the properties of $\boldsymbol{\alpha}$ derived in App. A to simplify the results.

Now we consider the second and fourth terms in Eq. (12). For the first parts of these two terms we approximate the times as before and then use the properties of P in App. A to simplify the result. Because of the h in the later terms we only need to keep the zeroth-order terms in the expansion. Therefore, we derive

$$\begin{aligned} \frac{P(x_r(t_r) - x_e(t_s), y_r(t_r) - y_e(t_s))}{\sqrt{(\mathbf{p}_R(t_r) - \mathbf{p}_E(t_s))^2}} &= \\ \frac{L^2}{t_1} P(\hat{x}, \hat{y}) + 2LP(\hat{x}, \hat{y}, v_x, v_y) + t_1 P(v_x, v_y), \end{aligned} \quad (22a)$$

$$\begin{aligned} \frac{P(x_e(t_e) - x_r(t_r), y_e(t_e) - y_r(t_r))}{\sqrt{(\mathbf{p}_E(t_e) - \mathbf{p}_R(t_r))^2}} &= \\ \frac{L^2}{t_2} P(\hat{x}, \hat{y}) - 2LP(\hat{x}, \hat{y}, v_x, v_y) + t_2 P(v_x, v_y). \end{aligned} \quad (22b)$$

For the second parts of the second and fourth terms, we expand the h analogous to Eqs. (15) and find that

$$i \frac{h^\omega(t_r, z_r(t_r)) - h^\omega(t_s, z_e(t_s))}{\omega(t_r - t_s) - k(z_r(t_r) - z_e(t_s))} = h^{\bar{\omega}}(t_s), \quad (23a)$$

$$i \frac{h^\omega(t_e, z_e(t_e)) - h^\omega(t_r, z_r(t_r))}{\omega(t_e - t_r) - k(z_e(t_e) - z_r(t_r))} = h^{\bar{\omega}}(t_s). \quad (23b)$$

Because we need \mathfrak{h}_1 and \mathfrak{h}_2 to complete the calculation, we revisit Eq. (14) and notice that $t_r - t_s$ equals to the sum of the first and second terms in Eq. (12), and that $t_e - t_r$ equals to the sum of the third and fourth terms.

From these two equations we find

$$\begin{aligned} \mathfrak{h}_1 = & \left[\frac{1}{2(1-v_z)} P(v_x, v_y) - \frac{\gamma(\theta)\hat{z}L}{t_1(1-v_z)} P(\hat{x}, \hat{y}, v_x, v_y) \right. \\ & \left. - \hat{z}L \frac{\gamma(\theta)\hat{z} + 1}{2t_1(1-v_z)^2} P(v_x, v_y) - \frac{\gamma(\theta)L}{2t_1} P(\hat{x}, \hat{y}) \right] h^{\bar{\omega}}(t_s), \end{aligned} \quad (24a)$$

$$\begin{aligned} \mathfrak{h}_2 = & \left[\frac{1}{2(1-v_z)} P(v_x, v_y) - \frac{\gamma(\theta)\hat{z}L}{t_2(1-v_z)} P(\hat{x}, \hat{y}, v_x, v_y) \right. \\ & \left. - \hat{z}L \frac{\gamma(\theta)\hat{z} - 1}{2t_2(1-v_z)^2} P(v_x, v_y) - \frac{\gamma(\theta)L}{2t_2} P(\hat{x}, \hat{y}) \right] h^{\bar{\omega}}(t_s). \end{aligned} \quad (24b)$$

Using $t_e - t_s = t_1(1 + \mathfrak{h}_1) + t_2(1 + \mathfrak{h}_2)$, Eqs. (19) and (20), as well as the properties of P in App. A, we find

$$\begin{aligned} t_e - t_s = & 2\gamma L_0 \left(1 + \frac{1}{2} \left[\frac{P(v_x, v_y)}{(1-v_z)} - \left(\frac{\gamma(\theta)}{\gamma} \right)^2 \right. \right. \\ & \left. \left. \times P(\hat{x} + \psi_x \hat{z}, \hat{y} + \psi_y \hat{z}) \right] h^{\bar{\omega}}(t_s) \right), \end{aligned} \quad (25)$$

where $\psi_{x,y} := v_{x,y}/(1-v_z)$.

The last equation is coordinate-dependent because it is expressed in coordinate time. To get a coordinate-independent expression, we use the following relation between the coordinate time and the proper time of the emitter (see App. C):

$$t_e - t_s = \gamma(\tau_e - \tau_s) + \gamma L_0 \frac{P(v_x, v_y)}{1-v_z} h^{\gamma\bar{\omega}}(\tau_s). \quad (26)$$

The term $\gamma\bar{\omega}$ in the last equation is the Doppler-shifted frequency, which a moving detector will perceive. Moreover, we have used the relationship $h^{\bar{\omega}}(t_s) = h^{\gamma\bar{\omega}}(\tau_s)$ between the GW amplitudes in different frames, which is accurate up to linear order of h . Finally, we find that the light-travel time, which a clock fixed at the emitter would measure, is

$$\begin{aligned} \tau_e - \tau_s = & 2L_0 \left(1 - \frac{1}{2} \left[\tilde{F}_+(\hat{\mathbf{p}}, \mathbf{v}) h_+^{\gamma\bar{\omega}}(\tau_s) \right. \right. \\ & \left. \left. + \tilde{F}_\times(\hat{\mathbf{p}}, \mathbf{v}) h_\times^{\gamma\bar{\omega}}(\tau_s) \right] \right), \end{aligned} \quad (27)$$

where \tilde{F}_+ and \tilde{F}_\times are two new response patterns, i.e.,

$$\tilde{F}_{+, \times}(\hat{\mathbf{p}}, \mathbf{v}) := \left(\frac{\gamma(\theta)}{\gamma} \right)^2 F_{+, \times}(\hat{x} + \psi_x \hat{z}, \hat{y} + \psi_y \hat{z}). \quad (28)$$

B. Velocity dependent response patterns

The response patterns in Eq. (28) differ in many ways from the classic ones in Eq. (5). This difference results from two independent effects. First, the special-relativistic contraction of the arm in the rest frame of the

source results in a factor in front of $F_{+, \times}$. The Lorentz factors enter as quadratic terms because the response patterns are quadratic equations of the length. Second, the general-relativistic wiggling of the emitter and reflector relative to the GW source leads to the additional terms in the arguments of the $F_{+, \times}$.

There are some special cases in which at least one of the above two effects vanishes. (i) There is no relative motion. In this case, Eq. (28) reduces to the so-called ‘‘antenna patterns’’ [42] and we recover the classical light travel time in Eq. (16). (ii) The arm is perpendicular to the motion so that it is not contracted. (iii) There is a relative motion but only in the z -direction, i.e. $\psi_x = \psi_y = 0$. As we have discussed previously, the velocity four-vector in this case is not affected by the GW so that the wiggling effect vanishes. (iv) The relative motion is in an arbitrary direction, but the detector has a special orientation such that the arm lies in the plane of the wave front, i.e. $\hat{z} = 0$. In this case, the emitter and the reflector encounter the same GW phase and hence they also wiggle in phase. We note that this is the case considered in Ref. [11], where the authors claimed that to linear order there is no effect of relative motion on GW amplitude.

To illustrate the behavior of our new response patterns, i.e., Eq. (28), we plot in Fig. 1 a special case where the motion is in the x -direction, i.e. $\mathbf{v} = (v, 0, 0)$. The arm formed by the emitter and reflector lies in the plane spanned by the z -axis and the angle bisector of the x - and y -axes and its position is described by the angle ϕ between the arm and the wave-vector, as measured in the rest frame of the source. Without a velocity, such an one-armed detector, by construction, would be blind to the $+$ -polarization. When there is a velocity, we find three remarkable features. First, the patterns can either increase or diminish for an increasing velocity; they are not monotonic functions of velocity. Second, the dependence on velocity is different for the two polarizations and for different position angles of the arm. Third, the detector responds to the $+$ -polarization when it starts moving, except for the case $\phi = 90^\circ$. The third feature applies also to the \times -polarization if we start from a different configuration in which the detector initially is blind to this polarization.

We emphasize that our approach allows us to find, in a unified way, two effects on GWs due to relative motion. First, we recover the well-known Doppler effect for GWs. Second, we find a different response of the detector to GWs, which will fundamentally change the observable signals, as we will elaborate in the next section.

IV. DETECTING THE BEAMING EFFECT

An interferometer (LIGO/Virgo/LISA) detects a passing GW by discerning, effectively, the difference in the light travel times along the two arms of the same length, L_0 , pointing in two different directions $\hat{\mathbf{p}}_1$ and

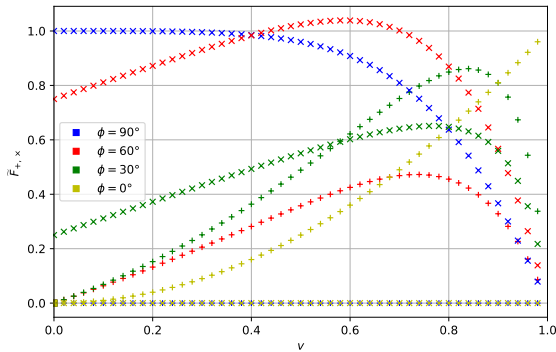


FIG. 1. Magnitudes of the two response patterns as a function of the velocity v . The plus symbols represent the pattern for the $+$ -polarization and crosses for the \times -polarization. In this example, the direction of the velocity is chosen to be along the x -axis. Both the emitter and the reflector lie in the plane spanned by the z -axis and the angle bisector of the x - and y -axes. The angle ϕ denotes the orientation of the arm relative to the wave-vector, as seen in the source frame.

\hat{p}_2 . This time difference $\delta\tau$, which is a function of the GW phase, is the only observable in GW observations and closely related to the amplitude of a GW signal, $h := \delta\tau/L_0$ [42, 44]. Because it is measured by a single clock placed at the intersection of the two arms, it is a proper time and Lorentz invariant.

We now know that given a waveform template computed in the rest frame of the source, one should use our response patterns, i.e. Eq. (28), to derive h if the source is moving relative to the observer. In contrast, if the observer is unaware of the relative motion and uses, instead, the classic antenna patterns, i.e. Eq. (5), to compute an amplitude h' , it will be different from h .

To understand the difference between h and h' , we study an ideal case in which the source is a circular binary and its sky location, inclination, and distance relative to the detector are known [38, 39]. We can set up a coordinate system as described at the beginning of the paper and compute the amplitudes of the signal using either Eq. (28) or Eq. (5). Moreover, we restrict our calculation to a representative example in which the relative velocity is in the x -direction. Furthermore, one arm is fixed in the y -direction, i.e., $\hat{p}_1 = (0, 1, 0)$, while the other rotates in the x - z -plane, i.e., $\hat{p}_2 = (\cos(\theta), 0, \sin(\theta))$. We choose this configuration because the fixed arm is not affected by the beaming effect while the rotating arm is. Under these circumstances, the two arms appear to be perpendicular to each other in both the source and the detector frame.

Finally, by varying the phase of GWs, we find that the maximum value for h is

$$h = h_0\epsilon_+ \left[1 + \frac{1 - v^2}{1 - v^2 \sin^2(\theta)} (\cos(\theta) + v \sin(\theta))^2 \right], \quad (29)$$

which an observer will take as the apparent magnitude of

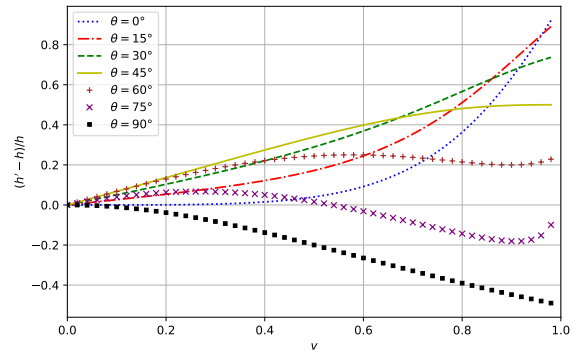


FIG. 2. Relative difference between h and h' (the amplitudes of the GW signal) as a function of the velocity v . Different curves refer to different orientations of the arm in the x - z plane. The amplitude of the signal h is calculated using our response patterns which account for the relative motion, while h' is calculated using the classic antenna patterns which are velocity-independent.

the GWs. Alternatively, using the velocity-independent antenna patterns in Eq. (5), we get

$$h' = h_0\epsilon_+ [1 + \cos(\theta)^2]. \quad (30)$$

Fig. 2 shows the relative difference between h and h' . In general, the difference is a function of the velocity and the orientation of the arms. Moreover, it is not always a monotonic function of the velocity, and when the velocity is fixed the difference can be either positive or negative depending on the orientation of the detector. We note that in the case of light, where the observable is flux and not amplitude, the beaming effect is, however, a monotonic function of velocity. Therefore, we find a fundamental difference between the beaming effect for light and that for GWs.

To understand the cause of the difference shown in Fig. 2, we first notice that for light the beaming effect can be fully explained by a Lorentz transformation of the wave-vector [36]. For GWs, we can also Lorentz transform the wave-vector into the detector frame, which, effectively, changes the relative angle between the wave-vector and our rotating arm. Placing this “corrected” angle in the classic antenna patterns while keeping the directions of the polarizations unchanged ($+$ -polarization aligned with the x, y -axes), we derive a new response of the detector:

$$h'_c = h_0\epsilon_+ \left[1 + (\cos(\theta)/\gamma + v \sin(\theta))^2 \right]. \quad (31)$$

This result is different from the h' derived in Eq. (30). The difference between h and h'_c is shown in Fig. 3. Although the difference vanishes in the case $\theta = 90^\circ$, it remains non-zero in the other cases. This result implies that the beaming effect, as we have seen in Fig. 2, cannot be attributed solely to the apparent change of the sky location of the source. In fact, the apparent directions of

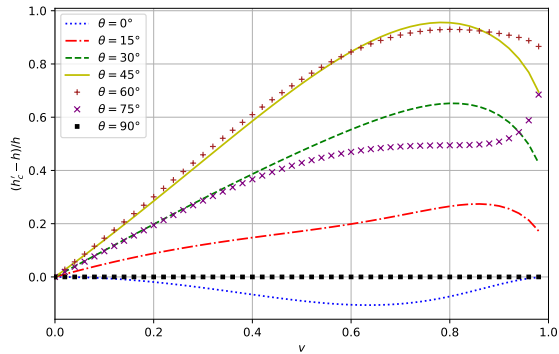


FIG. 3. The same as Fig. 2 but in the calculation of h' we correct the sky location of the source, as it is seen in the detector frame.

the polarizations also change [41]. Given the importance of the direction of GW polarization in the inference of the orientation of the source, we will study in a future work the effect induced by a relative motion on GW polarization, as well as its astrophysical implications.

So far, we have shown that ignoring the velocity of the source would result in a systematic error in the prediction of the GW signal. Fig. 4 shows this systematic error for relatively low velocities. We find that it is not negligible relative to the calibration accuracy of LIGO. For example, when one of the arms is perpendicular and the other tilted by $30^\circ - 75^\circ$ relative to the direction of the velocity, a motion of $(0.7 - 1.0)\%$ of c would already induce a systematic error that exceeds the best calibration accuracy of LIGO in the first and second observing runs [49]. For even higher velocities such as $0.1c$ [33–35], the systematic error could even exceed the upper limit of the calibration accuracy of LIGO. In the future, LIGO could further improve its calibration accuracy to $(0.2 - 1.0)\%$ [50, 51]. According to the same figure, even a velocities as small as 0.25% of c could cause a significant error in the measurement of the amplitude of GWs.

V. CONCLUSIONS

Despite the seminal work of Isaacson [52] which shows that the propagation of GWs is, in many aspects, similar to that of light, here we found that the beaming effect for GWs, i.e., the response of a detector to a moving source, is fundamentally different. First, the apparent amplitude of the GW signal, h , is not a monotonic function of the velocity. Second, the detector responds differently to the two polarizations when the velocity changes. Third, and most remarkably, the behavior of the signal can be explained partially, but not fully, by the special-relativistic effects known for light, such as time dilation, Doppler-shift, length contraction, and aberration. The missing link is the re-orientation of the polarization directions

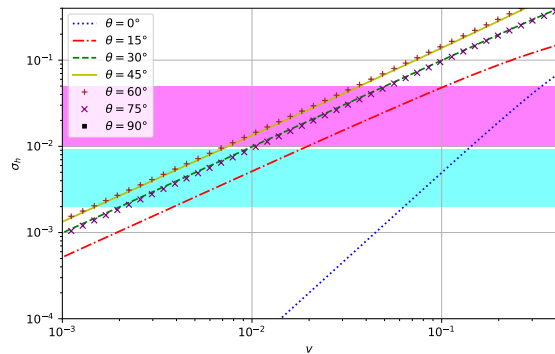


FIG. 4. Systematic error, $\sigma_h := |h'_c - h|/h$, in the prediction of GW signals as a function of v . The lines are adopted from Fig. 3. The magenta shaded area shows the calibration accuracy in the first and second LIGO observing runs. The cyan one shows the designated calibration accuracy for the future runs.

when there is a velocity. Because of the wide use of GW amplitudes to determine the distance of the source [53] and the polarizations to infer the orbital inclination [42] or test alternative gravity theories [43], our results will have important applications in the future for GW astrophysics and fundamental physics.

ACKNOWLEDGMENTS

We thank Leor Barack, Cliff Will, and Carlos Sopuerta for helpful discussions and suggestions. This work is supported by the “985 Project” of Peking University and the National Science Foundation of China (No. 11873022, 11690023, and 11622546). XC is partly supported by the Strategic Priority Research Program of the Chinese Academy of Sciences, Grant No. XDB23040100 and No. XDB23010200. PAS acknowledges support from the Ramón y Cajal Programme of the Ministry of Economy, Industry and Competitiveness of Spain, as well as the COST Action GWverse CA16104.

Appendix A: Some properties of α and P

For P , defined in Eq. (7), we have:

$$P(\lambda a, \lambda b) = \lambda^2 P(a, b), \quad (\text{A1a})$$

$$P(a + b, c + d) = P(a, c) + 2P(a, c, b, d) + P(b, d), \quad (\text{A1b})$$

where

$$P(a, b, c, d) := \epsilon_+(ac - bd) + \epsilon_\times(ad + bc), \quad (\text{A2})$$

which in turn fulfills

$$P(\lambda a, \lambda b, c, d) = P(a, b, \lambda c, \lambda d) = \lambda P(a, b, c, d). \quad (\text{A3})$$

For the α defined in Eq. (18), \mathbf{v} the relative velocity, and $\hat{\mathbf{p}}$ the direction of the arm, we find:

$$\mathbf{v} \cdot \alpha = -\frac{1}{2}(1-v_z)P(v_x, v_y) - \frac{P(v_x, v_y)}{2\gamma^2}, \quad (\text{A4a})$$

$$\hat{\mathbf{p}} \cdot \alpha = \frac{v \cos(\theta) - \hat{z}}{2}P(v_x, v_y) - (1-v_z)P(\hat{x}, \hat{y}, v_x, v_y). \quad (\text{A4b})$$

Appendix B: The geodesic of a moving particle

In this section we solve the geodesic of a test particle under the influence of GWs. We say the particle is initially at the point $\mathbf{p}_0 = (x_0, y_0, z_0)$ and moves with a velocity $\mathbf{v} = (v_x, v_y, v_z)$, whereas the GW source is far away and at rest. We apply the coordinate system and the metric introduced in Section II.

The geodesic equation for a point particle in a force free space is [47]

$$\ddot{x}^\alpha + \Gamma_{\beta\gamma}^\alpha \dot{x}^\beta \dot{x}^\gamma - \Gamma_{\beta\gamma}^0 \dot{x}^\beta \dot{x}^\gamma \dot{x}^\alpha = 0, \quad (\text{B1})$$

where we define $x^0 := t$ to write the geodesic equation in terms of the coordinate time, the dot denotes the coordinate time derivative, and $\Gamma_{\beta\gamma}^\alpha$ is the *Christoffel symbol*. Moreover, the geodesic of a massive particle has to fulfill the constraint

$$g_{\mu\nu} \dot{x}^\mu \dot{x}^\nu \left(\frac{dt}{d\tau} \right)^2 = 1, \quad (\text{B2})$$

where τ is the proper time along the geodesic (see App. C). For the metric in Eq. (1) the Christoffel symbols have the form

$$\Gamma_{\beta\gamma}^\alpha = -\frac{1}{2}i\omega h^\omega(t, z) \left[\epsilon_\beta^\alpha (\delta_\gamma^3 - \delta_\gamma^0) + \epsilon_\gamma^\alpha (\delta_\beta^3 - \delta_\beta^0) - \epsilon_{\beta\gamma} (\eta^{\alpha 3} - \eta^{\alpha 0}) \right], \quad (\text{B3})$$

where δ_β^α is the *Kronecker-Delta* and $\epsilon_{\mu\nu} := (h_{\mu\nu}|_{t,z=0})/h_0$.

We assume the velocity of the spatial coordinates \mathbf{p} can be separated into the initial velocity, \mathbf{v} , and a function $\mathbf{f} := (f_x, f_y, f_z)$ of order h describing the effect of the GW:

$$\dot{\mathbf{p}} = \mathbf{v} + \mathbf{f}. \quad (\text{B4})$$

Accordingly, $z(t) = z_0 + v_z t + g$, where g is a function fulfilling $\dot{g} = f_z$. Up to linear order in h the geodesic

equation is

$$\ddot{\mathbf{p}} + i\omega \alpha h^{\bar{\omega}}(t, z_0) = 0, \quad (\text{B5})$$

where α is introduced in Eq. (18). The general solution to the differential equation is

$$\mathbf{p}(t) = \mathbf{p}_0 + \mathbf{v}t + \frac{i\alpha h^{\bar{\omega}}(t, z_0)}{\bar{\omega}(1-v_z)}, \quad (\text{B6})$$

which also fulfills the constraint in Eq. (B2).

Considering the special case where the initial velocity vanishes, α is also zero and the geodesic reduces to

$$\mathbf{p}(t) = \mathbf{p}_0, \quad (\text{B7})$$

consistent with the classic notion that a particle at rest stays at rest in the TT-gauge.

Appendix C: Proper time along the geodesic

In this section we calculate the proper time along the geodesic derived in App. B. To linear order in h it is related to the coordinate time as

$$d\tau = \left(\frac{1}{\gamma} - \frac{1}{2} \frac{P(v_x, v_y)}{\gamma(1-v_z)} h^{\bar{\omega}}(t, z_0) \right) dt. \quad (\text{C1})$$

Integrating the left side from τ_a to τ_b and the right side from t_a to t_b we find

$$\tau_b - \tau_a = \frac{1}{\gamma}(t_b - t_a) + \frac{1}{2} \frac{P(v_x, v_y)}{\gamma \bar{\omega}(1-v_z)} \times i [h^{\bar{\omega}}(t_b, z_0) - h^{\bar{\omega}}(t_a, z_0)]. \quad (\text{C2})$$

For zero velocity, we recover that $\tau_b - \tau_a$ equals $t_b - t_a$, i.e., the proper time is the same as the coordinate time. For a non-vanishing velocity and neglecting the terms linear in h , $\tau_b - \tau_a$ equals $(t_b - t_a)/\gamma$. Rearranging Eq. (C2) we find

$$t_b - t_a = \gamma(\tau_b - \tau_a) - \frac{1}{2} \frac{P(v_x, v_y)}{\bar{\omega}(1-v_z)} \times i [h^{\gamma \bar{\omega}}(\tau_b, z_0) - h^{\gamma \bar{\omega}}(\tau_a, z_0)], \quad (\text{C3})$$

where we have used $t = \gamma\tau$ to replace t in the h .

To relate the coordinate time to the proper time along the geodesic of the emitter we proceed as follows: (i) we set $z_0 = 0$, (ii) t_a and t_b are replaced by t_s and t_e , respectively, and accordingly for the proper times, (iii) h can be expanded as in Eqs. (15), and (iv) for the times in h we can use $t_s = \gamma\tau_s$. Finally, we find Eq. (26).

[1] The LIGO Scientific Collaboration and the Virgo Collaboration, arXiv e-prints , arXiv:1811.12907 (2018), arXiv:1811.12907 [astro-ph.HE].
[2] The LIGO Scientific Collaboration and The Virgo Col-

laboration, arXiv e-prints , arXiv:1811.12940 (2018), arXiv:1811.12940 [astro-ph.HE].
[3] F. Pretorius, Phys. Rev. Lett. **95**, 121101 (2005), gr-qc/0507014.

- [4] M. Campanelli, C. O. Lousto, P. Marronetti, and Y. Zlochower, *Phys. Rev. Lett.* **96**, 111101 (2006), arXiv:gr-qc/0511048.
- [5] J. G. Baker, J. Centrella, D.-I. Choi, M. Koppitz, and J. van Meter, *Phys. Rev. Lett.* **96**, 111102 (2006), arXiv:gr-qc/0511103.
- [6] A. Buonanno and T. Damour, *Phys. Rev. D* **59**, 084006 (1999), gr-qc/9811091.
- [7] A. Buonanno, Y. Pan, J. G. Baker, J. Centrella, B. J. Kelly, S. T. McWilliams, and J. R. van Meter, *Phys. Rev. D* **76**, 104049 (2007), arXiv:0706.3732 [gr-qc].
- [8] P. Ajith, M. Hannam, S. Husa, Y. Chen, B. Brügmann, N. Dorband, D. Müller, F. Ohme, D. Pollney, C. Reisswig, L. Santamaría, and J. Seiler, *Physical Review Letters* **106**, 241101 (2011), arXiv:0909.2867 [gr-qc].
- [9] L. Santamaría, F. Ohme, P. Ajith, B. Brügmann, N. Dorband, M. Hannam, S. Husa, P. Mösta, D. Pollney, C. Reisswig, E. L. Robinson, J. Seiler, and B. Krishnan, *Phys Rev D* **82**, 064016 (2010), arXiv:1005.3306 [gr-qc].
- [10] C. Bonvin, C. Caprini, R. Sturani, and N. Tamanini, *Phys. Rev. D* **95**, 044029 (2017), arXiv:1609.08093.
- [11] D. Gerosa and C. J. Moore, *Physical Review Letters* **117**, 011101 (2016), arXiv:1606.04226 [gr-qc].
- [12] Y. Meiron, B. Kocsis, and A. Loeb, *Astrophys. J.* **834**, 200 (2017), arXiv:1604.02148 [astro-ph.HE].
- [13] K. Inayoshi, Z. Haiman, and J. P. Ostriker, *Mon. Not. R. Astron. Soc.* **459**, 3738 (2016), arXiv:1511.02116 [astro-ph.HE].
- [14] K. Chamberlain, C. J. Moore, D. Gerosa, and N. Yunes, *Phys. Rev. D* **99**, 024025 (2019), arXiv:1809.04799 [gr-qc].
- [15] J. Calderón Bustillo, J. A. Clark, P. Laguna, and D. Shoemaker, *ArXiv e-prints* (2018), arXiv:1806.11160 [gr-qc].
- [16] B. P. Abbott, R. Abbott, T. D. Abbott, M. R. Abernathy, F. Acernese, K. Ackley, C. Adams, T. Adams, P. Addesso, R. X. Adhikari, and et al., *Astrophysical Journal Letters* **818**, L22 (2016), arXiv:1602.03846 [astro-ph.HE].
- [17] P. Amaro-Seoane and X. Chen, *Mon. Not. R. Astron. Soc.* **458**, 3075 (2016), arXiv:1512.04897.
- [18] F. Antonini and H. B. Perets, *Astrophys. J.* **757**, 27 (2012), arXiv:1203.2938.
- [19] S. Prodan, F. Antonini, and H. B. Perets, *Astrophys. J.* **799**, 118 (2015), arXiv:1405.6029.
- [20] A. P. Stephan, S. Naoz, A. M. Ghez, G. Witzel, B. N. Sitarski, T. Do, and B. Kocsis, *Mon. Not. R. Astron. Soc.* **460**, 3494 (2016), arXiv:1603.02709 [astro-ph.SR].
- [21] J. H. VanLandingham, M. C. Miller, D. P. Hamilton, and D. C. Richardson, *Astrophys. J.* **828**, 77 (2016), arXiv:1604.04948 [astro-ph.HE].
- [22] B. Liu, Y.-H. Wang, and Y.-F. Yuan, *Mon. Not. R. Astron. Soc.* **466**, 3376 (2017), arXiv:1701.04580.
- [23] C. Petrovich and F. Antonini, *Astrophys. J.* **846**, 146 (2017), arXiv:1705.05848 [astro-ph.HE].
- [24] B. Bradnick, I. Mandel, and Y. Levin, *Mon. Not. R. Astron. Soc.* **469**, 2042 (2017), arXiv:1703.05796 [astro-ph.HE].
- [25] B.-M. Hoang, S. Naoz, B. Kocsis, F. A. Rasio, and F. Dosopoulou, *Astrophys. J.* **856**, 140 (2018), arXiv:1706.09896 [astro-ph.HE].
- [26] M. Arca-Sedda and A. Gualandris, *Mon. Not. R. Astron. Soc.* **477**, 4423 (2018), arXiv:1804.06116.
- [27] G. Fragione, E. Grishin, N. W. C. Leigh, H. B. Perets, and R. Perna, *arXiv e-prints*, arXiv:1811.10627 (2018), arXiv:1811.10627 [astro-ph.GA].
- [28] D. Syer, C. J. Clarke, and M. J. Rees, *Mon. Not. R. Astron. Soc.* **250**, 505 (1991).
- [29] J. M. Bellovary, M.-M. Mac Low, B. McKernan, and K. E. S. Ford, *Astrophys. J. Lett.* **819**, L17 (2016), arXiv:1511.00005.
- [30] I. Bartos, B. Kocsis, Z. Haiman, and S. Márka, *Astrophys. J.* **835**, 165 (2017), arXiv:1602.03831 [astro-ph.HE].
- [31] N. C. Stone, B. D. Metzger, and Z. Haiman, *Mon. Not. R. Astron. Soc.* **464**, 946 (2017), arXiv:1602.04226.
- [32] B. McKernan, K. E. S. Ford, J. Bellovary, N. W. C. Leigh, Z. Haiman, B. Kocsis, W. Lyra, M. M. Mac Low, B. Metzger, M. O’Dowd, S. Endlich, and D. J. Rosen, *Astrophys. J.* **866**, 66 (2018), arXiv:1702.07818 [astro-ph.HE].
- [33] X. Chen, S. Li, and Z. Cao, *ArXiv e-prints* (2017), arXiv:1703.10543 [astro-ph.HE].
- [34] X. Chen and W.-B. Han, *ArXiv e-prints* (2018), arXiv:1801.05780 [astro-ph.HE].
- [35] W.-B. Han and X. Chen, *ArXiv e-prints* (2018), arXiv:1801.07060 [gr-qc].
- [36] M. H. Johnson and E. Teller, *Proceedings of the National Academy of Sciences* **79**, 1340 (1982), <https://www.pnas.org/content/79/4/1340.full.pdf>.
- [37] J. D. Jackson, *Classical electrodynamics*, 3rd ed. (Wiley, New York, NY, 1999).
- [38] P. Peters and J. Mathews, *Physical Review (U.S.) Superseded in part by Phys. Rev. A, Phys. Rev. B: Solid State, Phys. Rev. C, and Phys. Rev. D* **131** (1963), 10.1103/PhysRev.131.435.
- [39] P. Peters, *Physical Review (U.S.) Superseded in part by Phys. Rev. A, Phys. Rev. B: Solid State, Phys. Rev. C, and Phys. Rev. D* **136** (1964), 10.1103/PhysRev.136.B1224.
- [40] W. H. Press, *Phys. Rev. D* **15**, 965 (1977).
- [41] K. S. Thorne, *Three Hundred Years of Gravitation*, edited by S. W. Hawking and W. Israel (1987) pp. 330–458.
- [42] B. S. Sathyaprakash and B. F. Schutz, *Living Reviews in Relativity* **12**, 2 (2009), arXiv:0903.0338 [gr-qc].
- [43] J. R. Gair, M. Vallisneri, S. L. Larson, and J. G. Baker, *Living Reviews in Relativity* **16**, 7 (2013), arXiv:1212.5575 [gr-qc].
- [44] B. Schutz, *A First Course in General Relativity by Bernard Schutz. Cambridge University Press, 2009. ISBN: 9780521887052* (Cambridge University Press, 2009).
- [45] LIGO Scientific Collaboration, J. Aasi, B. P. Abbott, R. Abbott, T. Abbott, M. R. Abernathy, K. Ackley, C. Adams, T. Adams, P. Addesso, and et al., *Classical and Quantum Gravity* **32**, 074001 (2015), arXiv:1411.4547 [gr-qc].
- [46] P. Amaro-Seoane, H. Audley, S. Babak, J. Baker, E. Barausse, P. Bender, E. Berti, P. Binétruy, M. Born, D. Bortoluzzi, J. Camp, C. Caprini, V. Cardoso, M. Colpi, J. Conklin, N. Cornish, C. Cutler, K. Danzmann, R. Dolesi, L. Ferraioli, V. Ferroni, E. Fitzsimons, J. Gair, L. Gesa Bote, D. Giardini, F. Gibert, C. Grimani, H. Halloin, G. Heinzl, T. Hertog, M. Hewitson, K. Holley-Bockelmann, D. Hollington, M. Hueller, H. Inchauspe, P. Jetzer, N. Karnesis, C. Killow, A. Klein, B. Klipstein, N. Korsakova, S. L. Larson, J. Livas, I. Lloro, N. Man, D. Mance, J. Martino, I. Mateos, K. McKen-

- zie, S. T. McWilliams, C. Miller, G. Mueller, G. Nardini, G. Nelemans, M. Nofrarias, A. Petiteau, P. Pivato, E. Plagnol, E. Porter, J. Reiche, D. Robertson, N. Robertson, E. Rossi, G. Russano, B. Schutz, A. Sesana, D. Shoemaker, J. Slutsky, C. F. Sopuerta, T. Sumner, N. Tamanini, I. Thorpe, M. Troebels, M. Vallisneri, A. Vecchio, D. Vetrugno, S. Vitale, M. Volonteri, G. Wanner, H. Ward, P. Wass, W. Weber, J. Ziemer, and P. Zweifel, ArXiv e-prints (2017), arXiv:1702.00786 [astro-ph.IM].
- [47] C. W. Misner, K. S. Thorne, and J. A. Wheeler, *Gravitation, by Charles W. Misner, Kip S. Thorne, and John Archibald Wheeler. ISBN: 978-0-691-17779-3. Princeton NJ: Princeton University Press, 2017.* (Princeton University Press, 2017).
- [48] D. E. Holz and S. A. Hughes, *Astrophys. J.* **629**, 15 (2005), astro-ph/0504616.
- [49] C. Cahillane, J. Betzwieser, D. A. Brown, E. Goetz, E. D. Hall, K. Izumi, S. Kandhasamy, S. Karki, J. S. Kissel, G. Mendell, R. L. Savage, D. Tuyenbayev, A. Urban, A. Viets, M. Wade, and A. J. Weinstein, *Phys. Rev. D* **96**, 102001 (2017), arXiv:1708.03023 [astro-ph.IM].
- [50] D. Tuyenbayev, S. Karki, J. Betzwieser, C. Cahillane, E. Goetz, K. Izumi, S. Kandhasamy, J. S. Kissel, G. Mendell, M. Wade, A. J. Weinstein, and R. L. Savage, *Classical and Quantum Gravity* **34**, 015002 (2017), arXiv:1608.05134 [astro-ph.IM].
- [51] Y. Inoue, S. Haino, N. Kanda, Y. Ogawa, T. Suzuki, T. Tomaru, T. Yamamoto, and T. Yokozawa, ArXiv e-prints (2018), arXiv:1804.08249 [astro-ph.IM].
- [52] R. A. Isaacson, *Phys. Rev.* **166**, 1263 (1967).
- [53] B. F. Schutz, *Nature (London)* **323**, 310 (1986).